World Journal of Advanced Research and Reviews
eISSN: 2581-9615 CODEN (USA): WJARAI
Cross Ref DOI: 10.30574/wjarr
Journal homepage: https://wjarr.com/

(RESEARCH ARTICLE)

Check for updates

Photocatalytic degradation of methylene blue dye under solar light irradiation by zinc oxide nanoparticles using aqueous extract of *Cleome gynandra*

V.VELMANI, P. RAJESH *, M. BALAJI, G.T. PARETHE and S. KAVICA

PG & Research Department of Chemistry, Government Arts College (Autonomous), (Affiliated to Bharathiar University), Coimbatore-641018, India.

World Journal of Advanced Research and Reviews, 2024, 22(02), 061–069

Publication history: Received on 20 March 2024; revised on 28 April 2024; accepted on 30 April 2024

Article DOI: https://doi.org/10.30574/wjarr.2024.22.2.1303

Abstract

A simple green synthetic technique is proposed for the synthesis of zinc oxide nanoparticles (ZnONPs) using the plant extract *Cleome gynandra* as a bio-template. The morphological, functional and structural characterization of synthesized ZnONPs was investigated using several techniques, such as energy dispersive X-ray analysis (EDX), scanning electron microscopy (SEM), X-ray diffraction (XRD) and UV-visible spectroscopy. The synthesized ZnONPs have a wurtzite hexagonal nanostructure with an average size of 15.20 nm. Furthermore, the photocatalytic degradation of methylene blue (MB) in an aqueous solution was carried out using the synthesized ZnONPs. The photocatalytic activity of ZnONPs was investigated by adjusting physicochemical variables as reaction time, medium pH, precursor concentration, and photocatalyst dosage. All results indicate that ZnONPs produced by the green approach exhibits significant photocatalytic activity against dye molecules.

Keywords: Green synthesis; Zinc oxide nanoparticles; Sunlight; Photocatalytic degradation; Methylene blue

1. Introduction

Effluents from dying, textile, paper, and agriculture sectors are highly contaminated with dyes, phenols, pesticides and heavy metals, posing severe health and environmental hazards. The existence of such chemicals in the environment, especially in water bodies, is an issue of concern both for society and regulatory authorities globally due to their resistance to natural decomposition. The majority of conventional water treatment techniques, including chemical treatment, adsorption, and membrane filtering, are inefficient at completely removing dyes. Conversely, secondary pollutants including hazardous gases and sludge are also produced by these methods as solid wastes that need to be further treated. Therefore, dye-contaminated effluent must be treated before it's discharged into the environment.

Environmental nanotechnology has become increasingly significant in the removal of hazardous pollutants and has the ability to promote economically viable synthesis. Nanoparticles (NPs) in nanotechnology are classified according to their shape, structure, size, and chemical properties [1, 2]. Metal oxide nanoparticles (NPs) are synthesized using a wide range of chemical and physical methods, like electro-explosion, solvothermal, hydrothermal, microwave, spray pyrolysis, vapour deposition, microemulsion, coprecipitation, and the wet-chemical approach [3-6]. However, the toxicity, expense, and production of various nanostructures associated with these conventional methods of NP synthesis restrict its applicability [3]. The advent of diverse production techniques for semiconductor nanoparticles has garnered significant attention in recent times [7, 8]. Green chemistry production of NPs addresses environmental problems by reducing harmful compounds and requiring minimal process investment [9, 10]. Plant extract-mediated synthesis is an affordable, effective, and viable approach due to the availability of phytochemicals and functional groups in the extractives [11].

* Corresponding author: P. RAJESH

Cleome gynandra (CG) belongs to *Cleomaceae (Capparaceae)* family, it is widely used medicinal herb available globally. In India, it is found in all states and grows naturally everywhere. Owing to the diverse range of nutrients and chemical components found in *Cleome gynandra*, they have multiple applications. Its therapeutic benefits were documented in Indian ayurvedic pharmacopoeia and other medical literature penned by prehistoric peoples across the world. The sap that was extracted from the leaves of the *Cleome gynandra* plant was used to cure epileptic fits, headaches, stomachaches, and earaches [12]. Additionally, it possesses antioxidant, antimicrobial, and anti-inflammatory properties [13-15].

Zinc oxide (ZnO) is a non-toxic metal oxide that can remove environmental pollutants through photodegradation, particularly in wastewater treatment [16-18]. ZnONPs have gained attention for their exceptional ability to degrade contaminants [19]. Modi and colleagues reported on employing zinc oxide nanoparticles and nanocomposites to remove MB dye from wastewater [20]. Modi et al. found that combining ZnONPs with a bacterial consortia can improve photocatalytic degradation efficiency for methylene blue dye [21].

The goal of the current work is to synthesize green zinc oxide nanoparticles (ZnONPs) using the extract of the *Cleome gynandra* plant and assessing their ability to photodegrade methylene blue (MB). The photocatalytic degradation of MB dye was examined with several physicochemical parameters, including reaction time, precursor concentration, medium pH and catalyst quantity.

2. Experimental method

All of the reagents and solvents were analytical grade and used without further purification. Zinc sulphate heptahydrate ($ZnSO_4.7H_2O$), Methylene blue, Sodium Hydroxide (NaOH) and Ethanol were purchased from Sigma Aldrich and Himedia chemicals, Coimbatore, India. The *Cleome gynandra* plant were collected from Rasipuram, Namakkal District, Tamil Nadu, India.

2.1. Preparation of plant extract

The fresh *Cleome gynandra* plants were collected, thoroughly washed with tap water, followed by distilled water and allowed to dry in a shed for 15 days. The completely dried plants were ground to a fine powder using a mixer grinder. About 10 g of fine powder was weighed and transferred to a 500 mL flask containing 250 mL of double-distilled water, which was then heated for 1 h at 60-80 ^{0}C using a magnetic stirrer. The solution was then filtered using Whatman filter paper No. 1 whereas the temperature was constantly maintained. The filtrate solution was used to synthesis ZnONPs, and the extract was stored in the refrigerator for further uses.

2.2. Synthesis of *CG*-ZnO nanoparticles

For the green synthesis of the *CG*-ZnONPs, 50 mL of plant extract and 100 mL of an aqueous solution of 0.1M Zinc sulphate heptahydrate ($ZnSO_4.7H_2O$) were stirred for 1 h. Sodium Hydroxide (NaOH) 1N solution was added drop wise into the mixture under stirring to maintain the pH value at 12. The resultant white precipitate was separated from reaction solution by centrifugation at 7000 rpm for 10 minutes by washing several times with distilled water followed by ethanol to remove organic impurities and dried in an oven 80 ^{0}C for 6 h. The dried sample was then stored for the characterization.

2.3. Characterization

The formation of zinc nanoparticles was confirmed by using a UV-Vis spectrophotometer (Perkin-Elmer lambda 19) to measure the wavelength absorption between 200 and 800 nm in order to assess the chemical components present in the samples. Using X-ray diffraction analysis, the crystalline properties, including average particle size, nature, and dimensions, were investigated. Scanning electron microscopy (SEM) and energy dispersive x-ray (EDX) spectrometer analysis were used to examine the surface morphology, such as shape, size, dispersed nature of nanoparticles, and elemental content of the synthesized sample.

2.4. Photocatalytic Studies on Methylene Blue Degradation

The photocatalytic experiment was carried out to investigate the photodegradation of MB dye in an aqueous solution under direct sunlight. 100 mL of MB dye (10–50 ppm) was prepared, and 5 mg/L of ZnONPs was added. Before photocatalytic degradation, the solution was stirred for 30 minutes in complete darkness to attain the adsorption–desorption equilibrium. Throughout the experiment, the 600 rpm stirring rate was maintained. The suspension was then exposed to sunlight while being constantly stirred to ensure that the photocatalyst was properly activated. Each sample was centrifuged at 5000 rpm for 10 min after being irradiated at a definite time interval to eliminate the

photocatalyst from the suspension. The residual MB concentration in the solution was measured using a UV-Vis spectrophotometer at 663 nm, followed by a wavelength scan between 200-800 nm. The percentage of photodegradation of MB (photocatalytic efficacy of ZnONPs) in aqueous medium was estimated using the following equations:

$$\text{Degradation Efficiency} = (C_0 - C_t) / C_0 \times 100 \quad (1)$$

where C_0 is the initial concentration of MB dye, C_t is the final concentration of MB dye after degradation.

3. Results and discussion

3.1. UV-visible Spectroscopy analysis

The UV-visible spectroscopy was used to analyze the synthesized *CG*-ZnONPs. The absorption spectra were identified within the wavelength range of 200–800 nm. A strong electronic absorption was observed at 355 nm (Fig. 1), consistent with the significant quantum confinement effect of ZnO particles [22]. The high excitation binding energy of ZnONPs at room temperature was centered at around 360 nm [23]

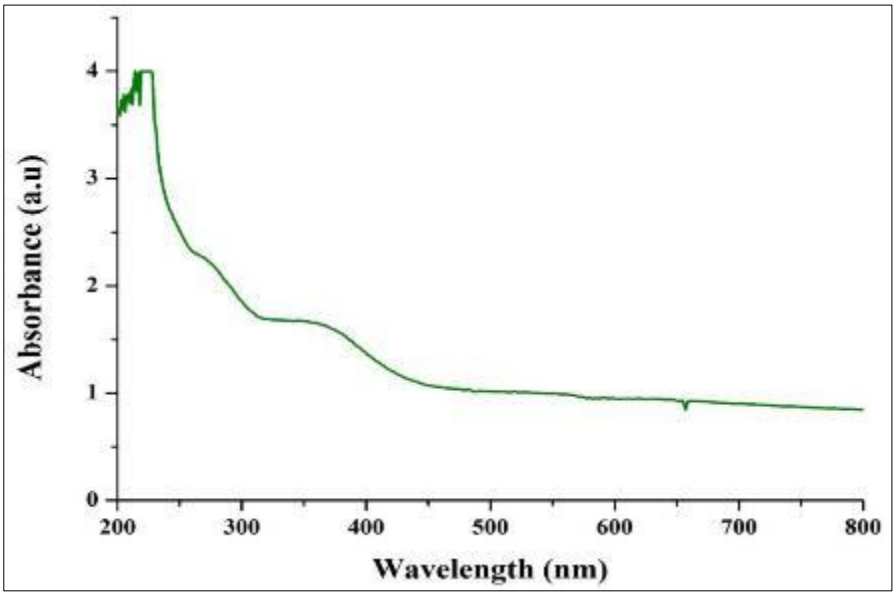

Figure 1 UV-visible spectra of green synthesized *CG*-ZnONPs

3.2. X-Ray Diffraction analysis

The X-ray diffraction method is used to determine the crystal lattice, phases, and planes of nanoparticles. The observed diffraction peaks at 2θ values of 31.33^0, 34.37^0, 47.11^0, 56.68^0, and 62.73^0 correspond to the Bragg's lattice plane of (100), (002), (101), (102), (110) and (103), respectively, with respect to "hkl" values (Fig. 2). The planes of the *CG*-ZnONPs diffraction pattern demonstrated that zinc was in the +2 oxidation state. Furthermore, the JCPDS card number 36-1451 [24] and the diffraction pattern matched well. The average crystalline size of the *CG*-ZnONPs measured using Debye Scherer's formula was 15.20 nm. The crystal structure of the *CG*-ZnONPs was found to be wurtzite hexagonal, as previously reported [25].

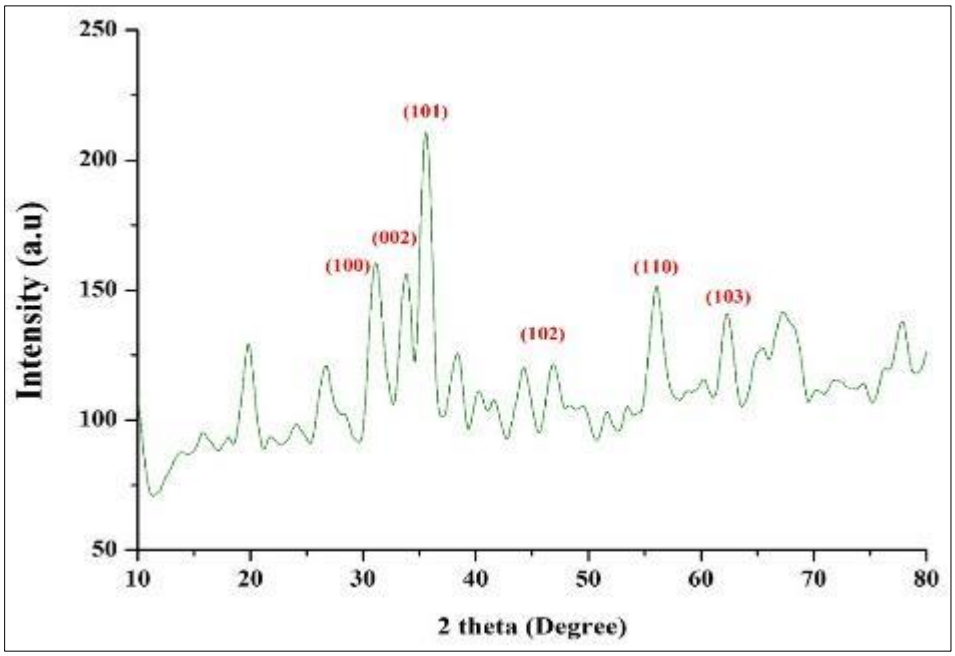

Figure 2 XRD pattern of green synthesized *CG*-ZnONPs

3.3. Energy Dispersive X-ray (EDX) and Scanning Electron Microscopy (SEM) analysis

The synthesized CG-ZnONPs are illustrated in Fig. 3(a), whereas EDX measurements confirm the characteristic zinc and oxygen peaks at around 1 keV and 0.5 keV, respectively. Figure 3(b) displays the weight percentage distribution of the elements in the nanomaterial. A prominent carbon peak indicates the formation of scaping structures as a result of biomolecules associated with plant extracts. Figure. 4 shows a SEM image of ZnONPs obtained from a *C. gynandra* plant extract. Furthermore, the particles were discovered to be significantly agglomerated, which could have been caused by the materials' subsequent centrifugation and heating for SEM preparations.

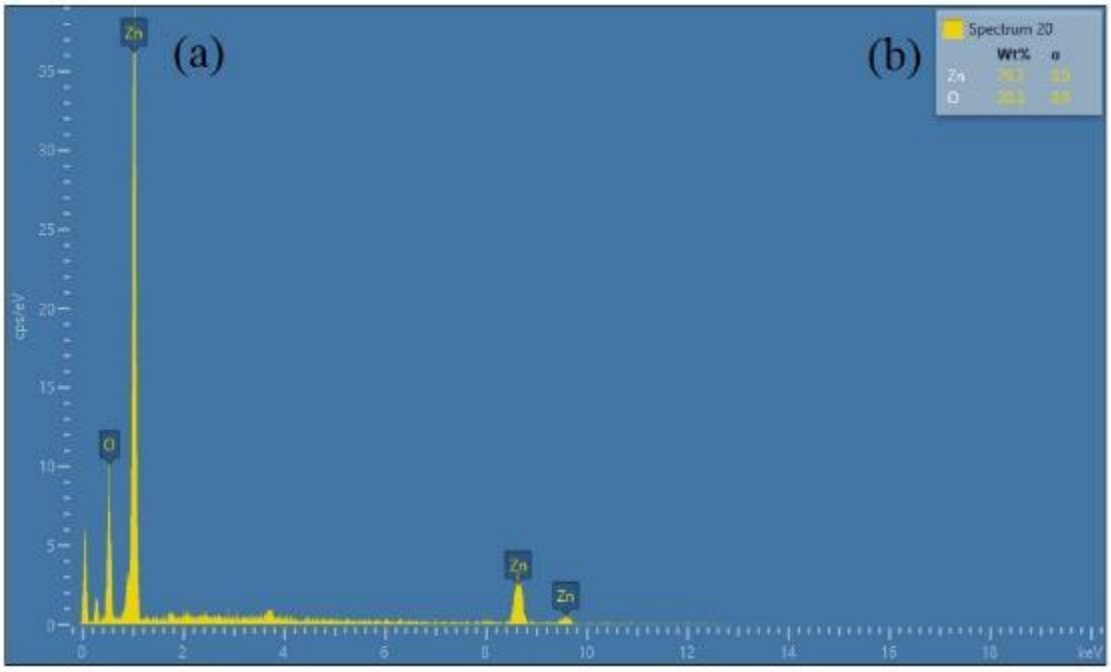

Figure 3 (a) EDX pattern and (b) Weight % distribution of elements in green synthesized *CG*-ZnONPs

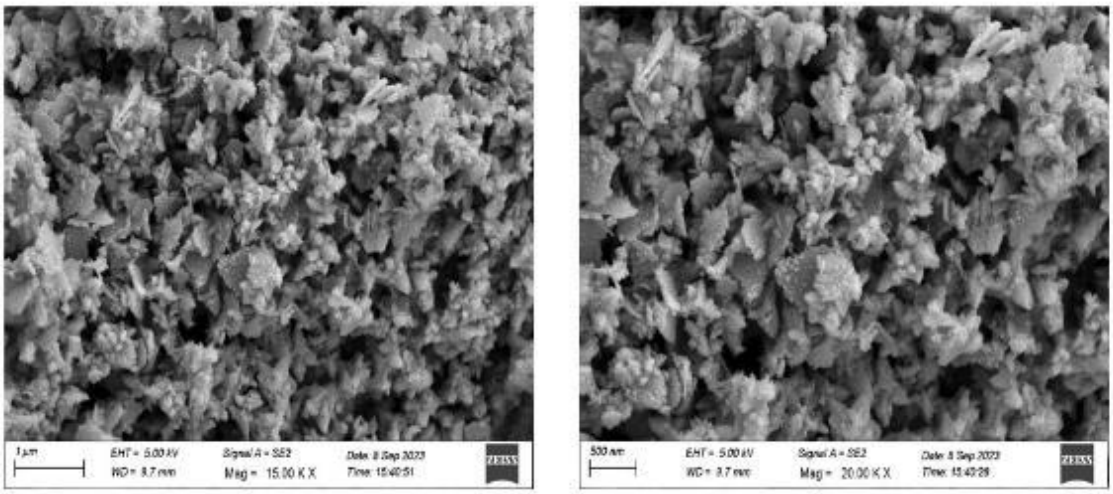

Figure 4 SEM image of green synthesized *CG*-ZnONPs

3.4. Effect of irradiation Time on Photodegradation of MB

The photocatalytic activity of ZnO nanoparticles has been evaluated by photodegrading MB organic pollutant dye(20 ppm) after 30 minutes of equilibrium. The influence of solar radiation on the percentage dye degradation of MB is shown in Figure. 5(a, b), which displays the absorption band for every sample at various time intervals (15,30,45,60,75,90,105,120), measured by loading ZnO catalyst in the presence of sunlight. In UV-visible spectra, the dye showed a distinct absorption peak at 663 nm. The efficiency that was calculated (34, 51, 56, 64, 68, 69, 76, 85 %) by examining the mixture's absorption during the time interval (15,30,45,60,75,90,105,120).

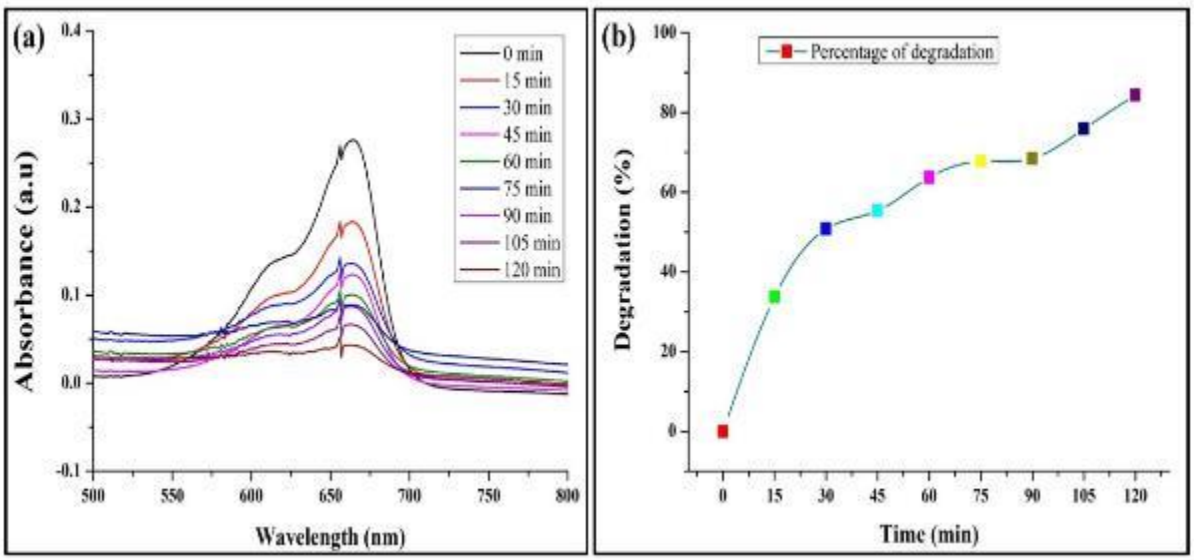

Figure 5 Effect of irradiation time interval on the photocatalytic degradation of MB dye and (b) percentage degradation of MB dye at 120 min

3.5. Effect of Catalyst dosage on Photodegradation of MB

The effect of the catalyst dosage on photocatalytic degradation of MB dye was investigated by adding 5-25 mg/100 mL of ZnO catalyst to the MB solution (20 ppm); the UV-visible spectra of the resulting solution are shown in Figure 6(a, b). The graph shows that the amount of catalyst has a significant impact on MB degradation. As the catalytic dosage was increased from 5 mg to 25 mg, the percentage of MB dye degradation increased from 50.15% to 58.25%.

The effect of increased percentage degradation is most likely attributable to more catalytic active sites, a larger adsorption area, and a larger specific surface area [26, 27]. Surface defects enhance the specific surface area that can be

used by active radicals to degrade the dye. However, an increase in catalyst quantity only resulted in an 8% improvement in photocatalytic efficiency. This may be due to particle aggregation, which increases the turbidity of the suspension as a result of high photocatalyst dosages [28].

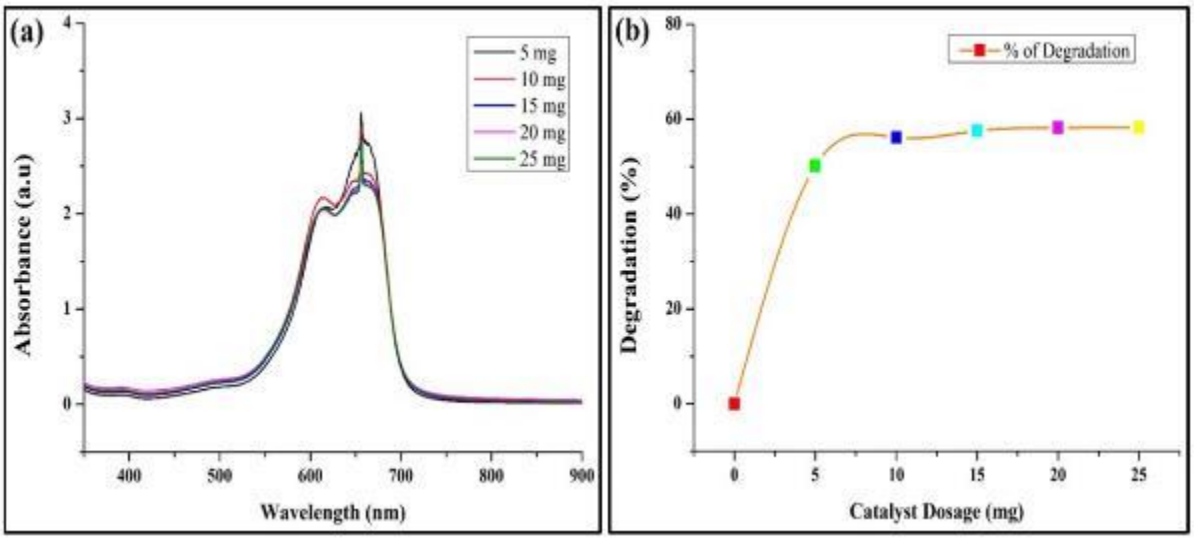

Figure 6 Effect of dosage of nano-photocatalyst on the photocatalytic degradation of MB dye and (b) percentage degradation of MB dye at 120 min

3.6. Effect of pH value on Photodegradation of MB

The pH of a solution is crucial for photocatalytic degradation of organic pollutants like dyes. It also affects the formation of hydroxyl radicals [29]. As pH increased, the percentage of dye degradation increased. Fig. 7 (a, b) shows that Mb dye degradation was most effective at pH 10, with ~92% degradation in 120 min. Higher pH levels can increase the number of hydroxyl ions that react with holes, leading to faster dye decolorization.

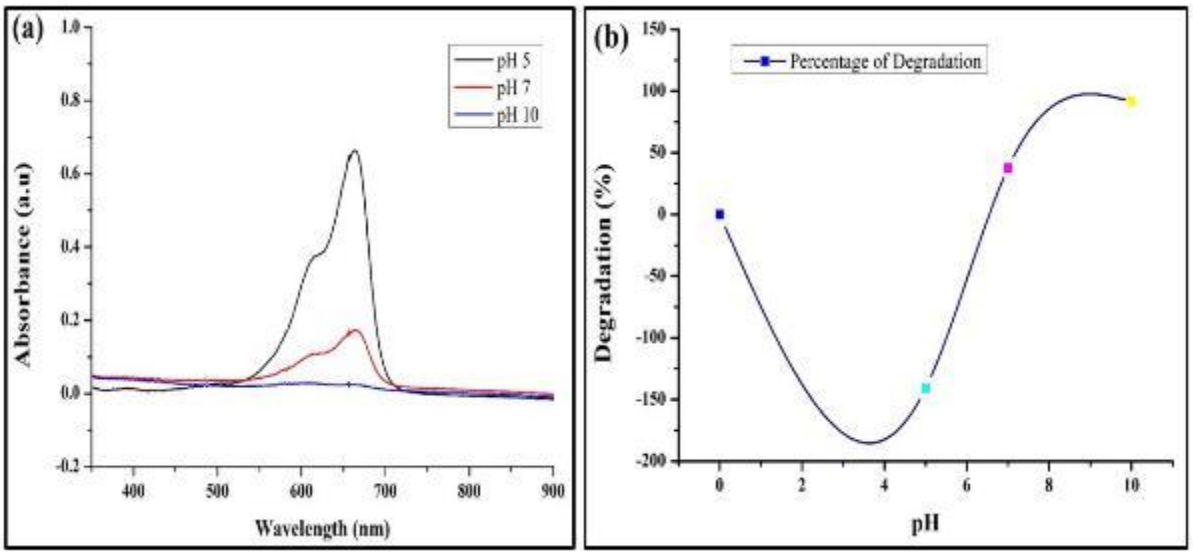

Figure. 7 (a) Effect of pH on the photocatalytic degradation of MB dye and (b) percentage degradation of MB dye at 120 min

3.7. Effect of Concentration of the dye on Photodegradation of MB

The effect of initial dye concentrations on the degradation efficiency of the MB was studied as well by varying the MB concentration from 10 to 50 ppm under direct sunlight irradiation while keeping the photocatalyst dose constant at 5 mg. Figure 8(a, b) shows the results of photocatalytic data graphically. The results obtained revealed that the ZnO

nanoparticle's photocatalytic activity is inversely related to the dye concentration under similar conditions, i.e., the maximum degradation efficacy was measured at the lowest MB concentration (10 ppm).

When the concentration of MB was increased from 10 to 50 ppm, the degradation of MB decreased from 93.31% to 50.67%. This reduction is caused by a decrease in light absorption on the photocatalyst surface as a result of an increase in dye concentration. This, in turn, limits the formation of $OH^{\bullet}$ radical ions, which are vital to the photodegradation process. The obtained results indicate that the catalyst's degrading efficiency is maximum when the MB dye concentration is 10 ppm.

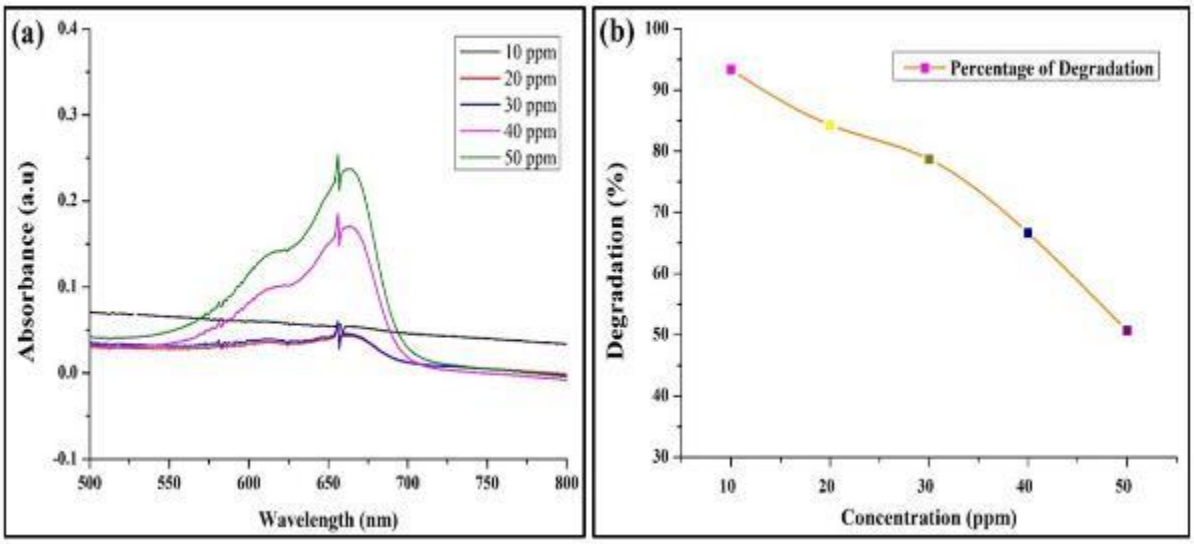

Figure 8 Effect of concentration of the dye on the photocatalytic degradation of MB dye and (b) percentage degradation of MB dye at 120 min

4. Conclusion

Green synthesis of ZnONPs using the *Cleome gynandra* template is a simple, stable, feasible, economical, and sustainable alternative to conventional methods. The *C. gynandra* extract's phytochemicals were crucial in the synthesis process because they acted as capping agents. The synthesized ZnONPs were wurtzite hexagonal crystalline in nature, with an average size of 15.20 nm. The produced material was evaluated as a photocatalyst under the direct sunlight for degradation of methylene blue dye, a hazardous industrial effluent. The photocatalyst showed excellent degradation efficacy at pH 10, with ~92% degradation in 120 min. observably, the photocatalytic activity of ZnONPs stabilized by *C. gynandra* was entirely dependent on various factors and optimal catalytic performance conditions. In addition, it was found that pH 7 and pH 10 are optimal for the best catalytic activity and that the photocatalyst can be used effectively for the degradation of MB dye in the concentration range of 10 to 20 ppm. The results of this investigation remarkably suggest that green synthesized ZnONPs exhibit a maximum photocatalytic degradation capability of 92% for organic dye degradation. Therefore, the currently employed method offers an excellent replacement for alternative methods and can be developed for use in large-scale operations for the treatment of wastewater and purification of water.

Compliance with ethical standards

Disclosure of conflict of interest

No conflict of interest to be disclosed.

References

[1] Zare, E.N.; Padil, V.V.T.; Mokhtari, B.; Venkateshaiah, A.; Wacławek, S.; C˘ erník, M.; Tay, F.R.; Varma, R.S.; Makvandi, P. Advancesin Biogenically Synthesized Shaped Metal- and Carbon-Based Nanoarchitectures and Their Medicinal Applications. Adv. Colloid Interface Sci. 2020, 283, 1–17. [CrossRef]

[2] Hebbalalu, D.; Lalley, J.; Nadagouda, M.N.; Varma, R.S. Greener Techniques for the Synthesis of Silver Nanoparticles Using Plant Extracts, Enzymes, Bacteria, Biodegradable Polymers, and Microwaves. ACS Sustain. Chem. Eng. 2013, 1, 703–712. [CrossRef]

[3] Mohammadinejad, R.; Karimi, S.; Iravani, S.; Varma, R.S. Plant-Derived Nanostructures: Types and Applications. Green Chem. 2015, 18, 20–52. [CrossRef]

[4] Kim, C.S.; Moon, B.K.; Park, J.H.; Choi, B.C.; Seo, H.J. Solvothermal Synthesis of Nanocrystalline TiO2 in Toluene with Surfactant. J. Cryst. Growth 2003, 257, 309–315. [CrossRef]

[5] Goti´c, M.; Musi´c, S. Synthesis of Nanocrystalline Iron Oxide Particles in the Iron(III) Acetate/Alcohol/Acetic Acid System. Eur. J. Inorg. Chem. 2008, 6, 966–973. [CrossRef]

[6] Hayashi, H.; Hakuta, Y. Hydrothermal Synthesis of Metal Oxide Nanoparticles in Supercritical Water. Materials 2010, 3, 3794–3817. [CrossRef]

[7] Yadav, A.; Burak, G.; Ahmadivand, A.; Kaushik, A.; Cheng, G.J.; Ouyang, Z.;Wang, Q.; Yadav, V.S.; Mishra, Y.K.;Wu, Y.; et al. Controlled Self-Assembly of Plasmon-Based Photonic Nanocrystals for High Performance Photonic Technologies. Nano Today2021, 37, 101072. [CrossRef]

[8] Vabbina, P.K.; Sinha, R.; Ahmadivand, A.; Karabiyik, M.; Gerislioglu, B.; Awadallah, O.; Pala, N. Sonochemical Synthesis of a Zinc Oxide Core-Shell Nanorod Radial p-n Homojunction Ultraviolet Photodetector. ACS Appl. Mater. Interfaces 2017, 9, 19791–19799. [CrossRef] [PubMed]

[9] Devatha, C.P.; Thalla, A.K. Green Synthesis of Nanomaterials. In Synthesis of Inorganic Nanomaterials; Elsevier: Amsterdam, The Netherlands, 2018; pp. 169–184.

[10] Padil, V.V.T.; Wacławek, S.; C˘ erník, M.; Varma, R.S. Tree Gum-Based Renewable Materials: Sustainable Applications in Nanotechnology, Biomedical and Environmental Fields. Biotechnol. Adv. 2018, 36, 1984–2016. [CrossRef]

[11] Kumar, M.D.K.R.A. Green Chemistry and Engineering, 1st ed.; Academic Press: Cambridge, MA, USA, 2007.

[12] Mishra, S.S., Moharana, S.K., Dash, M.R., 2011. Review on Cleome gynandra. Int. J. Res. Pharm. Chem. 1 (3), 681–689.

[13] Sridhar, N., Sasidhar, D.T., Kanthal, L.K., 2014. In vitro antimicrobial screening of methanolic extracts of Cleome chelidonii and Cleome gynandra. Bangladesh J. Pharmacol. 9 (2), 161–166.

[14] Narendhirakannan, R.T., Kandaswamy, M., Subramanian, S., 2005. Anti-inflammatory activity of Cleome gynandra L. on hematological and cellular constituents in adjuvant-induced arthritic rats. J. Med. Food 8 (1), 93–99.

[15] Moyo, M., Aremu, A.O., 2020. Nutritional, phytochemical and diverse health-promoting qualities of Cleome gynandra. Crit. Rev. Food Sci. Nutr. 1–18.

[16] Rastogi, A.; Zivcak, M.; Sytar, O.; Kalaji, H.M.; He, X.; Mbarki, S.; Brestic, M. Impact of Metal and Metal Oxide Nanoparticles on Plant: A Critical Review. Front. Chem. 2017, 5, 1–16. [CrossRef]

[17] Sabir, S.; Arshad, M.; Chaudhari, S.K. Zinc Oxide Nanoparticles for Revolutionizing Agriculture: Synthesis and Applications. Sci. World J. 2014. [CrossRef]

[18] Khalafi, T.; Buazar, F.; Ghanemi, K. Phycosynthesis and Enhanced Photocatalytic Activity of Zinc Oxide Nanoparticles toward Organosulfur Pollutants. Sci. Rep. 2019. [CrossRef]

[19] Widiyandari, H.; Ketut Umiati, N.A.; Dwi Herdianti, R. Synthesis and Photocatalytic Property of Zinc Oxide (ZnO) Fine Particle Using Flame Spray Pyrolysis Method. J. Phys. Conf. Ser. 2018, 1025. [CrossRef]

[20] Modi, S.; Yadav, V.K.; Gacem, A.; Ali, I.H.; Dave, D.; Khan, S.H.; Yadav, K.K.; Rather, S.-U.; Ahn, Y.; Son, C.T.; et al. Recent and Emerging Trends in Remediation of Methylene Blue Dye fromWastewater by Using Zinc Oxide Nanoparticles. Water 2022, 14, 1749. [CrossRef]

[21] Modi, S.; Yadav, V.K.; Amari, A.; Osman, H.; Igwegbe, C.A.; Fulekar, M.H. Nanobioremediation: A bacterial consortium-zinc oxide nanoparticle-based approach for the removal of methylene blue dye from wastewater. Environ. Sci. Pollut. Res. 2023, 30, 72641–72651. [CrossRef] [PubMed]

[22] V. Velmani et al. / J. Environ. Nanotechnol. , Vol. 13(1), 162-171 (2024).

[23] M. Mohammadian, Z. Eshaghi and S. Hooshmand, *J. Nanomed. Res.*, 7, 00175 (2018).

[24] F. Fan, Y. Feng, P. Tang, A. Chen, R. Luo and D. Li, *Ind. Eng. Chem. Res.*, 53, 12737 (2014).

[25] M. Darroudi, Z. Sabouri, R.K. Oskuee, A.K. Zak, H. Kargar and M.H.N. Abd Hamid, *Ceram. Int.*, 40, 4827 (2014).

[26] Chijioke-Okere, M.O.; Okorocha, N.J.; Anukam, B.N.; Oguzie, E.E. Photocatalytic Degradation of a Basic Dye Using Zinc Oxide Nanocatalyst. Int. Lett. Chem. Phys. Astron. 2019, 81, 18–26. [CrossRef]

[27] Ram, C.; Pareek, R.K.; Singh, V. Photocatalytic Degradation of Textile Dye by Using Titanium Dioxide Nanocatalyst. Int. J. Theor. Appl. Sci. 2012, 4, 82–88.

[28] Bansal, P.; Sud, D. Photodegradation of Commercial Dye, Procion Blue HERD from Real Textile Wastewater Using Nanocatalysts. Desalination 2011, 267, 244–249. [CrossRef]

[29] Isai KA, Shrivastava VS (2019) Photocatalytic degradation of methylene blue using ZnO and 2% Fe–ZnO semiconductor nanomaterials synthesized by sol–gel method: a comparative study. SN Appl Sci 1(10):1247